Colloid Polym Sci 280:365–371 (2002)

ORIGINAL CONTRIBUTION

Eduardo Humeres
N.A. Debacher

Kinetics and mechanism of coal flotation

Received: 6 August 2001
Accepted: 19 September 2001

E. Humeres (✉) · N.A. Debacher
Departamento de Química
Universidade Federal de Santa Catarina
88040-900 Florianópolis, SC, Brazil
e-mail: humeres@mbox1.ufsc.br
Tel: +55-48-3319219; Fax: +55-48-3319711

Abstract The flotation kinetics of coarse coal particles was studied in a modified version of the Hallimond tube at 25 °C using nitrogen as the carrier gas, in the pH range 2–12. The kinetics was followed by measuring the volume of the particles accumulated in the collector tube as a function of time. At each pH, the rate constants were determined at several buffer concentrations and were extrapolated to zero buffer concentration. The observed first-order rate constant was represented as the product of separable constants and functions such as f_D, f_V and f_{pH}, which depend only on the particle size, gas flow and the pH of the dispersion, respectively. The diameter, D, of the particles was in the range 505–127 μm. The observed rate constant decreased linearly with the diameter of the particles at constant flow and it was calculated that $f_D = \exp(-1.56D)$. The dependence of f_V on the flow is a consequence of the fact that the flotation occurs when a single particle is captured by two bubbles. f_V was shown to be independent of the particle diameter. The effect of the pH on the rate of flotation was considered as resulting from the adsorption of protons (or hydroxide ions) by the particles and bubbles through multiple equilibria, assuming that there is no interaction between the binding sites. The pH–rate profile showed that there were two species responsible for the flotation: one stable at pH below 5 and the other at high pH. Comparison of f_V, f_D and f_{pH} for the flotation of coal and pyrite allowed the prediction of the optimum conditions for the separation of mixtures of these particles by flotation.

Keywords Flotation · Flotation kinetics · Flotation mechanism · Coal flotation

Introduction

There are remarkable resemblances between flotation and chemical reactions. The simplest process occurs by the collision of particles and bubbles, which form a stable particle–bubble aggregate that rises to the surface of the solution. The main physical parameters that determine the rate of the process are the particle size, gas flow and pH.

The flotation rates of fine particles are in good agreement with the theoretically calculated collision rates [1], but the flotability is slow owing to the lower probability of collision between the particle and air bubbles [2, 3]. Attempts to develop theoretical relationships between the flotation rate and the particle size have been unsuccessful because other factors are also important contributors to the rate, such as the relative velocities of particles and bubbles [3] and their surface charges [4], which are determined at least in part by the pH of the dispersion. The complexity of the flotation process has not yet permitted the development of a quantitative description of the overall rate data.

Coarse particles with diameters in the range 100–500 μm are commonly found in many flotation processes, and for these particles the process of attachment to an air bubble [5] is limited by the acceleration of the particle–bubble complex, because if it exceeds a critical value, the particle will detach [6].

The rate of formation of stable bubble–particle aggregates follows Eq. (1):

$$dN_p/dt = kN_b^m N_p^n \quad , \tag{1}$$

where N_b and N_p are the instantaneous concentrations of bubbles and particles, and m and n are the respective orders of the kinetics process [7]. The order in this case indicates the number of elementary species involved in the rate-determining step and provides an insight into the mechanism of the process. For a complex system of several components, the flotation occurs as a competitive process, and the rate constant for each component determines the efficiency of the separation.

The rate constant, as defined in Eq. (1), is a complex function that depends on experimentally measurable properties of the system, such as the particle size, air flow and pH. It has been proposed that the observed rate constant, which contains all variables involved in the process, can be expressed as a factorised function, where each factor depends on a single variable as shown in Eq. (2) [8]:

$$k_{obs} = k_g k_i f_D f_V f_{pH} \quad . \tag{2}$$

k_g depends on the geometry of the Hallimond tube, on the stirring and the size and porosity of the sintered glass plate, which determine the number of bubbles [9]. k_i is determined by the intrinsic characteristics of the system, such as the shape and the hydrophobicity of the particle surface; f_V, f_D and f_{pH} are functions that depend only on the gas flow, the particle diameter, D, and the pH of the dispersion, respectively.

The flow rate, V, of the gas injected through a plate of a given porosity produces a number, n_b, of bubbles per unit time, with a mean volume $\bar{v}_b$. The concentration of bubbles, N_b, rising through the flotation media, is given by Eq. (3):

$$N_b = V \frac{\tau}{\bar{v}_b \bar{v}_d} \quad , \tag{3}$$

where V is the gas flow and τ is the average residence time of a bubble in the zone of flotation, v_d, where the dispersion of the particles is confined before the attachment to the bubbles.

Following this approach, the spontaneous flotation of coarse pyrite particles was found to be first order with respect to the number of particles; it showed a third-order dependence V, and depended exponentially on D, the mean diameter of the particles. The pH–rate profile showed a maximum at pH 7. When the gas flow varied in the range 0.50–1.2 lmin^{-1}, the results suggested that each particle undergoes a rapid sequence of "sticky" collisions with bubbles, forming a final aggregate containing an average of three bubbles, which is in equilibrium with other aggregates [8]. When the gas flow was in the range 100–300 mlmin^{-1}, the observed first-order rate constant increased linearly with the gas rate and with the increase in the mean volume of the bubbles ($\bar{v}_b = 1.05 - 6.4\,\mu$l at constant bubble concentration. The observed increase in the rate constant with $\bar{v}_b$ was ascribed to the increase in the probability of effective collisions that formed stable particle–bubble aggregates [9]. In the relatively wide range of the variables studied (V, D and pH), the product of the rate constants k_g k_i was remarkably constant, showing that the rate constant of flotation can, in effect, be factored as assumed in Eq. (2).

Selective flotation is considered to be one of the most promising techniques for coal desulfurization, particularly in the case of fine coal particles [10]. In this work, we studied the spontaneous flotation of coarse particles of coal and we applied the method described earlier in order to gain insight into the mechanism of coal flotation. A modified version of the Hallimond tube and a sensitive detection system [11] allowed measurement of the rate constant of flotation of coal particles of different sizes under a variety of controlled conditions, such as gas flow, porosity of the glass plate and pH.

Experimental

Materials

All the chemicals were of analytical grade and were used without further purification. The electrolytes and buffer solutions were prepared using distilled deoxygenated water. The pH was determined with a Metrohm Herisau model E603 pH meter, using a Metrohm 9100 Herisau combination electrode.

Coal samples were selected from Carbonífera Prospera, Mina A, Criciuma, in Santa Catarina, Brazil, and were kept in sealed plastic bags at −10 °C. The samples were reduced to about 5 mm in size using a porcelain mortar and were then pulverized in a Fritsch pulverizer and classified in a sieve shaker. The different fractions were also stored in sealed bottles at −10 °C. The coal was analysed as containing 23.8% ash, 27.7% volatiles, 48.6% carbon and 1.70% total sulfur.

Kinetics

The kinetics measurements were performed in a modified version of the Hallimond tube inserted in a setup as described in previous work [8, 11]. The mechanical stirring was maintained at 710 rpm. The nitrogen, used as a carrier and maintained at 25 °C, passed through a calibrated flowmeter before entering the Hallimond tube. A pressure equalizer allowed the kinetics run to start at the appropriate pressure.

The sample (0.5 g) was washed several times with distilled water to eliminate fine material adhering to the mineral surface, and then it was spread over the porous sintered glass plate of the Hallimond

tube using a small volume of buffer solution. The upper part of the Hallimond tube was then put into place and more buffer solution was added to make a total of 50 ml. The mineral and the buffer solution were allowed to equilibrate for 10 min.

The kinetics of flotation was followed by measuring the volume of mineral accumulated in the collector tube as a function of time. To ensure homogeneous sedimentation and the maximum packing of the floated particles, an ultravibrator was connected to the collector tube of the Hallimond tube. For each pH, the rate constants were determined at several buffer concentrations (10–100 mM) and were extrapolated to zero buffer concentration. Owing to the fast flotation and low density of the coal particles, the experiments were carried out as follows:

1. The initial reading of the floated volume was taken after allowing the carrier gas to flow for 5 s. The flow was stopped and the initial floated volume, V_0, was read.
2. The carrier flow was reinitiated until approximately 30% of the sample was floated, and the floated volume, V_1, was obtained.
3. A new pulse of carrier was injected in order to float about 70% of the sample, and the volume V_2 was obtained.
4. Finally, the carrier was allowed to flow until the entire sample was floated, and the total volume, V_∞, was obtained.

The observed rate constant, k_{obs}, was obtained from Eq. (4):

$$k_{obs} = \frac{1}{\Delta t}\ln\left(\frac{V_\infty - V_0}{V_\infty - V_0 - V_t}\right) \quad , \tag{4}$$

where V_0, V_∞ and V_t are the floated volumes at time $t_0 = 5$ s, infinity and time t respectively, and $\Delta t = t - t_0$. The value of k_{obs} was obtained from the average of 3–8 experiments, depending on the standard deviation.

Results and discussion

The batch flotation of pyrite was found to follow first-order kinetics with respect to the number of particles per unit volume, [8, 10] as shown in Eq. (5):

$$-\frac{dN_p}{dt} = k_{obs}N_p \quad . \tag{5}$$

Similar results have been obtained for other particles [12] under other experimental conditions, allowing us to assume that coal will also float following the same rate equation; therefore, $n = 1$ in Eq. (1).

Effect of particle size

A series of experiments were carried out by changing the size of the coal particles in the range of mean diameters 505–127 μm and the flow of the gas carrier between 0.2 and 1.0 lmin^{-1} (Fig. 1). k_{obs} decreases linearly with the increase in the mean diameter of the particles, at constant flow. For particles with constant mean diameter, the dependence of k_{obs} on the flow of the carrier follows an S-shaped curve (Fig. 2).

According to Eq. (2), the linear relationship between k_{obs} and D can be written as Eq. (6):

$$k_{obs} = k_g k_i f_V f_{pH}(1 + aD) \quad , \tag{6}$$

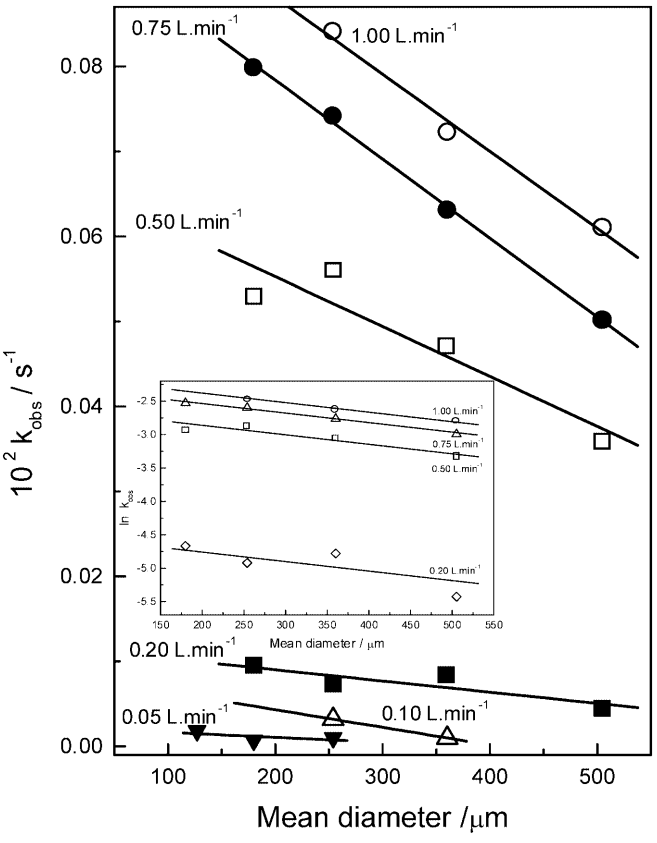

Fig. 1 Flotation rate constants of coal versuss mean diameter of particles at different flows of carrier gas at 25 °C; pH 6 (succinate 50 mM); stirring 710 rpm. *Insert*: lnk_{obs} versus D; the *lines* were all drawn with slope –1.56

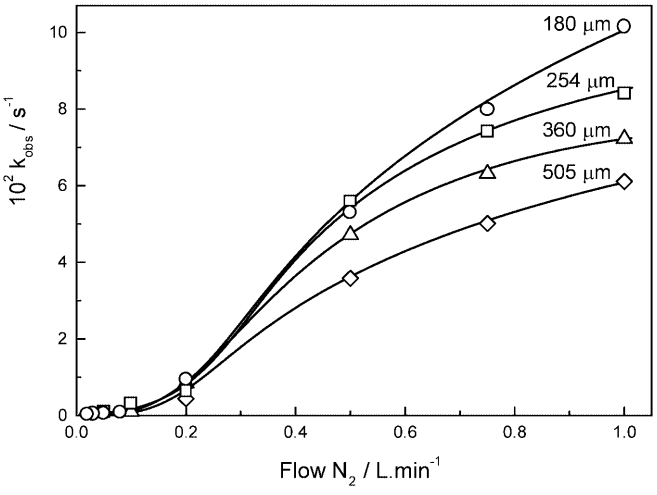

Fig. 2 Flotation rate constants of coal versus flow of the carrier gas at 25 °C using particles with different mean diameters; pH 6 (succinate 50 mM); stirring 710 rpm. The *curves* were calculated from Eq. (11) including f_D

where the parentheses can be considered as a series expression of the exponential function $\exp(aD)$ as shown in Eq. (7):

$$k_{obs} = k_g k_i f_v f_{pH} \exp(aD) \quad . \tag{7}$$

Consequently, a plot of $\ln k_{obs}$ versus D should be linear with constant slopes for different values of the gas flow. In the insert of Fig. 1, the straight lines were drawn with slope -1.56, and therefore $f_D = \exp(-1.56D)$. According to Eq. (2), the ratio k_{obs}/f_D is equal to $k_g k_i f_V f_{pH}$ or $k' f_V$ and should be independent of the particle diameter. This important result can be observed in Fig. 3, where the set of curves obtained for different values of D (Fig. 2) becomes only one curve when k_{obs}/f_D is plotted for different values of V.

The small standard deviations show that the system follows Eq. (2) under these experimental conditions.

Effect of gas flow

The dependence of k_{obs} on f_V and on the concentration of bubbles cannot be explained if the flotation simply occurs when a single particle is captured by a single bubble.

The steady-state concentration of stable bubble–particle aggregates rising through the flotation media depends on V, the gas flow, and the experimental value of the concentration of bubbles, N_b; this is surprisingly constant under different conditions of porosities, the height of the column and the gas flow rate [9]. Equation (8) assumes that coal particles need two bubbles to be floated:

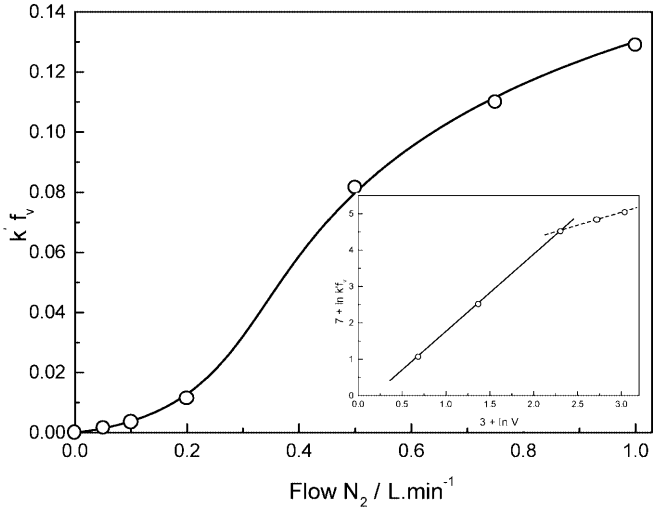

Fig. 3 Flow function $k' f_V$ versus the flow of the carrier gas. The *points* were calculated from Eq. (7) as the average for different particle diameters. *Insert*: Plot of $\ln k' f_V$ versus $\ln V$

$$C_n \underset{k_{-1}}{\overset{k_1 N_b}{\rightleftharpoons}} CB \underset{k_{-2}}{\overset{k_2 N_b}{\rightleftharpoons}} CB_2 \xrightarrow{k_3} C_f \tag{8}$$

C_n and C_f are the nonfloated and floated coal particles, respectively, and CB is the aggregate of one particle with one bubble and CB_2 that with two bubbles, and these are formed with rate constants k_1 and k_2, respectively. By applying the steady-state approximation to CB and CB_2, the observed rate constant is given by Eq. (9):

$$k_{obs} = \frac{k_1 k_2 k_3 N_b^2}{k_{-1}(k_{-2} + k_3) + (k_2 k_3 + k_1 k_{-2} + k_1 k_3) N_b + k_1 k_2 N_b^2} \quad . \tag{9}$$

Since N_b is constant and the rate constants k_1 and k_2 increase proportionally to $\bar{v}_b$ or V and can be substituted for $k'V$ and kV [9], Eq. (9) can then be written as Eq. (10):

$$k' f_V = \frac{V^2}{K_1 + K_2 V + K_3 V^2} \quad , \tag{10}$$

where

$$K_1 = \frac{k_{-1}(k_{-2} + k_3)}{k' k'' k_3 N_b^2} \quad ,$$

$$K_2 = \left(\frac{1}{k'} + \frac{k_{-2}}{k' k_3} + \frac{1}{k} \right) \frac{1}{N_b} \quad ,$$

$$K_3 = \frac{1}{k_3} \quad .$$

An iterative program of successive approximation was used to calculate the constants. The continuous line of Fig. 3 was calculated for $K_1 = 1.86$, $K_2 = 0$ and $K_3 = 5.65$. Equation (10) is reduced to Eq. (11):

$$k' f_V = \frac{V^2}{K_1 + K_3 V^2} \quad . \tag{11}$$

The set of curves of Fig. 2, which includes the function f_D, was calculated from Eq. (11). The ln–ln plot shown in the insert of Fig. 3 indicates, as expected from Eq. (11), that at low flow the order of the process with respect to the bubbles is 2, while at high flow it decreases because the increase in the mean volume of the bubbles allows some of the particles to float with only a single bubble.

Effect of pH

The rate constants were obtained at different pH at several buffer concentrations. The effect of the buffer is complex: the rate either increases or decreases with the concentration, and the change is only linear when the range is small (10–50 mM). When the pH is the only variable, the observed rate constant becomes equal to

$k''f_{pH}$ (Eq. 2) and can be expressed as the relative rate constant $k_{rel} = f_{pH}/f_7$ of the ratio between the value of the rate constant at any pH and the value at pH 7.0.

The pH–rate profile of the relative rate constants extrapolated to zero buffer concentration (Fig. 4) shows a plateau in the range of pH 2–4 and then it decreases to a minimum at pH 7, followed by a rapid increase at higher pH. The surface groups of the coal can be represented as *X*OH, but can also be a surface impurity group such as Si–OH or Al–OH. The change in pH can create positive sites by adsorption of H^+ ions or negative ones via deprotonation by OH^- ions [13]. Both processes will change the surface charge density and the surface potential. The pH profile can be interpreted by assuming that the coal particles float in the region of pH 2–4 owing to the protonation of a surface site with pK^+. The rate constants decrease at higher pH until the deprotonation of a second surface site with pK^- produces a rapid increase in the rate constants. For these two processes, k_{rel} can be expressed by Eq. (12), as proposed in previous work [8].

$$k_{rel} = \frac{k_n \left(\frac{a_H}{K^+}\right)^n + k_m \left(\frac{K^-}{a_H}\right)^m}{P_n + Q_m + 1} \quad , \tag{12}$$

where

$$P_n = \frac{a_H}{K^+}\left[\frac{1-\left(\frac{a_H}{K^+}\right)^n}{1-\left(\frac{a_H}{K^+}\right)}\right] \quad \text{and} \quad Q_m = \frac{K^-}{a_H}\left[\frac{1-\left(\frac{K^-}{a_H}\right)^m}{1-\left(\frac{K^-}{a_H}\right)}\right] .$$

The values of $pK^+ = 5.80$, $pK^- = 14.08$, $k_n = 1.35 \times 10^{-5}$, $k_m = 1.95 \times 10^{-4}$, $n = 0.52$ and $m = 0.23$ were calculated by a successive approximation program.

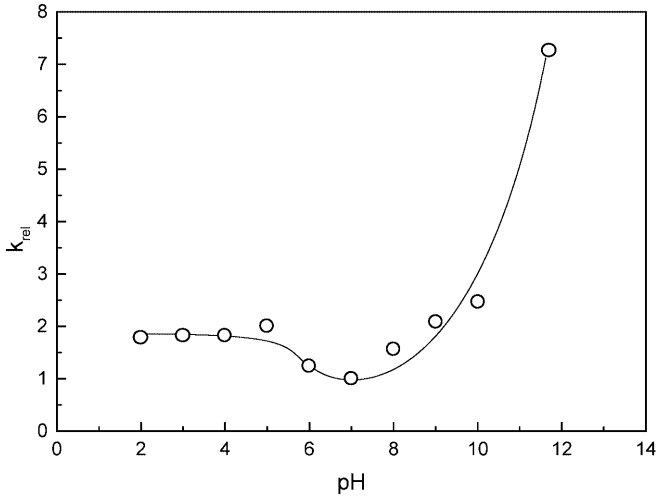

Fig. 4 Relative rate constants of flotation versus pH at 25 °C; $D = 254$ μm; stirring 710 rpm; $V = 0.2$ lmin^{-1}. The rate constants were extrapolated to zero buffer concentration and divided by the value at pH 7. The *continuous line* was calculated from Eq. (12)

The continuous curve of Fig. 4 was drawn with these values.

$k'f_V$ (Eq. 11) was obtained at pH 6.0 using succinate as the buffer, and therefore $k' = k_g k_i f'_6$. The product of $k'f_V k_{rel} f_D$ is equal to Eq. (13),

$$k'f_V k_{rel} f_D = k_g k_i f_V f_D f_{pH}\left(\frac{f'_6}{f_7}\right) = k_{obs}\left(\frac{f'_6}{f_7}\right) \quad , \tag{13}$$

which is equal to Eq. (2), except for the constant factor f'_6/f_7. The factor $f = (f_7/f_{6'}) = 0.320$ was calculated by considering $k'f_V$ for $V = 0.2$ lmin^{-1}, f_D for $D = 254$ μm and the value of k_{obs} at pH 6 (zero buffer concentration). The observed rate constant extrapolated to zero buffer concentration for the flotation of coal can then be written as Eq. (14):

$$k_{obs} = f\left(\frac{V^2}{K_1 + K_3 V^2}\right)\exp(a\overline{D}) \times \left\{\frac{k_i^+ \left(\frac{a_H}{K^+}\right)^n + k_i^- \left(\frac{K^-}{a_H}\right)^m}{\frac{a_H}{K^+}\left[\frac{1-(a_H/K^+)^n}{1-(a_H/K^+)}\right] + \frac{K^-}{a_H}\left[\frac{1-(K^-/a_H)^m}{1-(K^-/a_H)}\right]}\right\} . \tag{14}$$

It should be noted that k_n and k_m were substituted by k_i^+ and k_i^-, respectively, because k_{rel} depends only on the pH and the intrinsic characteristics of the surface represented by k_i. In the case of coal, the protonated and deprotonated particles present different flotability. On the other hand, k_g becomes undetermined as a consequence of the form of the f_V function, where K_1 and K_3 can be any multiple of k_g.

Comparison of the functions f_D, f_V and f_{pH} for the flotation of coal and pyrite

We can compare the independent effect of particle size, flow of carrier gas and pH on the relative rates of flotation of a mixture of coal and pyrite particles [8].

The plot of $\ln f_D$ versus D (Fig. 5) indicates that the ratio of the rate constants of the flotation of coal and pyrite decreases rapidly with D, as is known to occur forfines [10]. For a mixture of particles of different sizes, coal particles of 600 μm would float at the same rate as pyrite particles of 70 μm, if all the other factors were the same.

f_V for pyrite is compared with $k'f_V$ for coal as in Eq. (11) or as $V^2/(1 + K_3V^2/K_1)$ for different flow rates of the carrier in Fig. 6. Independent of the relative values of K_1 and K_3 for a flow lower than 0.4–0.5 lmin^{-1}, f_V for pyrite is lower than $k'f_V$, as has been observed experimentally [10]. At higher flow, the pyrite particles would float faster, other factors being the same.

Finally, in Fig. 7 a comparison is made between f_{pH} for pyrite [8] and f_{pH} for coal, calculated from Eq. (12) as k_{rel}/k_n. Even though the relative position between both

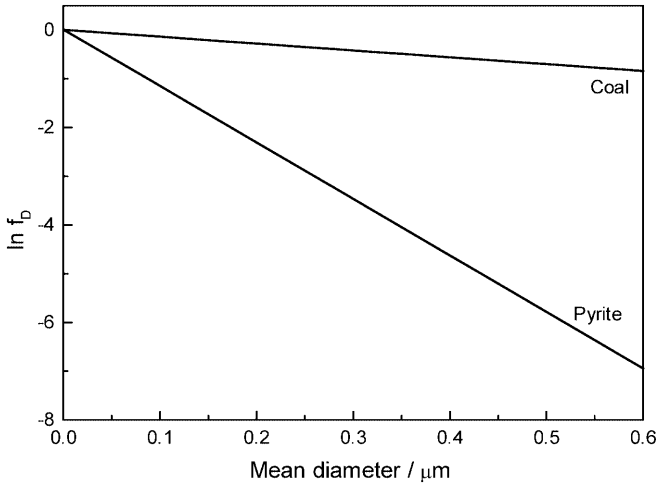

Fig. 5 Comparison of the f_D functions for the flotation of coal and pyrite

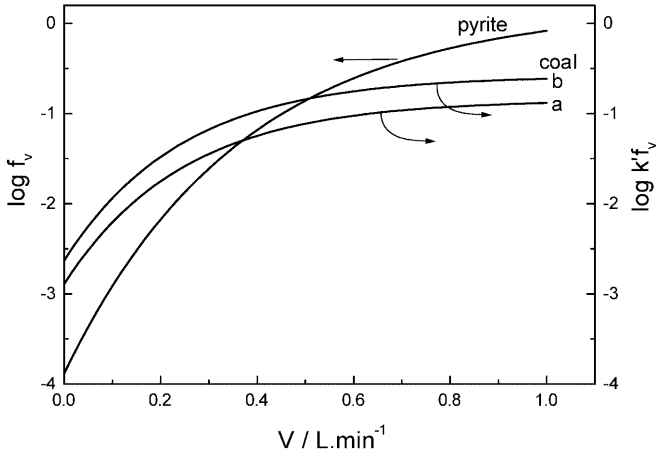

Fig. 6 Comparison of the f_V functions for the flotation coal and pyrite; *a* $k'f_V$ as in Eq. (11); *b* $k'f_V = V^2/(1 + K_3V^2/K_1)$

curves may change, it still predicts that coal should float faster than pyrite at higher pH. Accordingly, Zimmerman [14] showed that the sulfur content in floated coal decreases when the pH increases from 4 to 11.

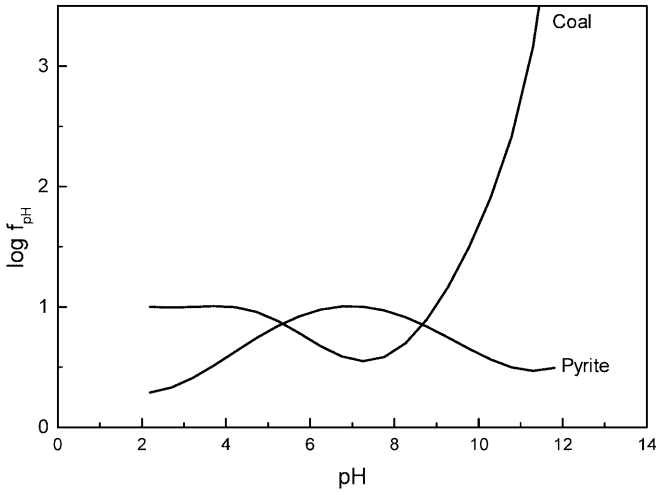

Fig. 7 Comparison of the f_{pH} functions for the flotation of coal and pyrite. For coal, f_{pH} was drawn as k_{rel}/k_n

Conclusions

The observed first-order rate constant k_{obs} of flotation of coarse particles of coal is proportional to the product $f_D f_V f_{pH}$, which contains functions that depend only on the particle size, gas flow and the pH of the dispersion. The flotation of a single coal particle occurs when it is captured by two bubbles. Bubble–particle aggregates are stable in the range of pH 2–5 and at high pH.

Comparison of the independent effect of particle size, flow of carrier gas and pH on the flotation of a mixture of coal and pyrite particles allows the prediction of the conditions to increase the relative rates of flotation and these rates are consistent with data from the literature.

Acknowledgements This work was finished during the stay of E.H. at the Institute of Fundamental Research of Organic Chemistry of Kyushu University, as Visiting Professor. We thank Shinjiro Kobayashi for the invitation.

References

1. (a) Ives KJ (1984) The scientific basis of flotation. Nijhoff, The Hague; (b) Anfruns JF, Kitchener JA (1977) Inst Min Met c9–c15
2. (a) Reay D, Ratcliff GA (1973) Can J Chem Eng 51:178–185; (b) Flint LR, Howarth W (1971) J Chem Eng Sci 26:1155–1168; (c) Trahar WJ, Warren LJ (1976) Int J Miner Process 3:103–131
3. Sutherland KL (1948) J Phys Colloid Chem 52:394–425
4. (a) Collins GL, Jameson GL (1977) Chem Eng Sci 32:239–246; (b) Schulze HJ, Cichos C (1972) Z Phys Chem 251:252–68
5. Schulze HJ (1977) Int J Miner Process 4:241–259
6. Jowett A (1980) In: Fine particle processing. Proceedings of the international symposium on fine particles, Las Vegas, Nev
7. Tewari SN, Biswas AK (1969) J Appl Chem 19:173–177
8. Humeres E, Gonzales G, Dias Filho NL, Debacher NA, Sierra MM de S (1992) J Braz Chem Soc 3:1–7

9. Humeres E, Debacher NA, Wagner T (1999) Colloids Surf A 149:595–601
10. Aplan FF (1977) In: Wheelock TD (ed) Coal desulfurization. Chemical and physical methods. ACS symposium series. American Chemical Society, Washington, DC
11. Humeres E, Debacher NA, Wagner T (1993) Sep Sci Technol 28:1515–1521
12. Collins GL, Jameson GL (1976) Chem Eng Sci 31:985–991
13. Hamieh T, Siffert B (1994) Colloids Surf A 84:217–228
14. Zimmerman RE (1948) Trans AIME 117:338–341